

Complete Wetting on "Strong" Substrates: Xe/Pt(111)

Klaus Kern, Rudolf David, Robert L. Palmer, and George Comsa

Institut für Grenzflächenforschung und Vakuumphysik, Kernforschungsanlage Jülich, D-5170 Jülich, West Germany
(Received 6 March 1986)

The growth of Xe films on Pt(111) has been investigated by elastic and inelastic, high-resolution, thermal-He scattering. Down to 25 K, Xe films grow layer by layer up to at least 25-monolayer films. This enlarges the complete wetting range on the so-called "scale of substrate strength" by a factor of 4. A buckling of the rotated monolayer has been observed for the first time. This demonstrates that the full monolayer is locked on the substrate and suggests that orientational ordering contributes to complete wetting on strongly binding substrates.

PACS numbers: 68.45.Gd, 68.35.Bs, 68.55.Ce, 79.20.Rf

The recent studies on the wetting behavior of physisorbed films have been just reviewed.¹ Two main types of growth of multilayer films on solid surfaces have been observed so far: "type 1" or "complete wetting," in which the film grows layer by layer, its surface remaining uniformly flat during the whole growing process; "type 2" or "incomplete wetting," in which the film is uniformly flat only for a limited number of monolayers (typically one or two) up to bulk coexistence. The wetting behavior has been rationalized by the introduction of an improved "scale of substrate strength"^{2,3}; the substrate strength is defined as the ratio of the isosteric heat of adsorption of the gas molecules onto the substrate surface at low coverages, u_1 , to the 0-K cohesive energy of the bulk phase of the gases, h_0 .³ One of the central but unexpected conclusions deduced from experiments is that incomplete wetting appears to be the universal type of growth; complete wetting is restricted at low temperatures to a very narrow range of substrate strengths.^{2,3} Only Ar, Kr, and Xe have been found to exhibit complete wetting on graphite. Most of these investigations being performed on graphite, experiments on other substrates have been asked for (see Ref. 3). The type-2 behavior of these and other gases observed on Au(111), a much stronger substrate, seems to give additional support to the universality of this behavior.⁴

Weak interaction with the substrate has been recognized for a long time as the cause for incomplete wetting. The discovery of incomplete wetting also for strong interaction with the substrate, the so-called reentrant incomplete wetting, and the suggestion that strong substrate attraction leads to high-density first layers and thus to a lattice mismatch between first layers and bulk-phase structures^{2,3} have triggered pertinent theoretical work. Three papers which appeared almost simultaneously⁵⁻⁷ confirm this suggestion and reach similar conclusions; in particular, that complete wetting occurs only when "the net stress tending to strain the film parallel to the substrate vanishes."⁵ The stress, which on strong substrates tends to compress the film, especially the monolayer,⁵ is recog-

nized as the cause for the reentrant incomplete wetting on these substrates. In this context, it is surprising that the Novaco-McTague orientational ordering⁸ has not been considered so far as a possible contribution to a reduction of the substrate-induced strain energy of the monolayer. Indeed, the rotation of monolayers with respect to the symmetry directions of the substrate observed for a number of systems has been predicted by Novaco and McTague to be caused by the tendency to minimize the strain energy. Fuselier, Raich, and Gillis⁹ have reached similar conclusions, and showed in addition that the equilibrium configurations of the rotated monolayers are higher-order commensurate, with a fraction of the adatoms sitting in energetically favorable high-symmetry sites.

We demonstrate here that down to 25 K (the lowest temperature accessible in this experiment) Xe exhibits type-1 behavior on Pt(111) up to at least 25 ML (ML=monolayer). Pt is a much stronger substrate than graphite (low-coverage Xe isosteric heat of adsorption $u_1/k_B \approx 3200$ K,¹⁰ compared to 2260 K³ on graphite). Accordingly, the type-1 behavior range on the scale of substrate strength defined in Ref. 3 is increased by a factor of 4. If one accepts that the monolayer rotation reduces substantially the strain energy there is no real contradiction with the type-2 behavior seen on Au(111).⁴ Indeed, no monolayer rotation seems to take place on Au(111), probably because of the $\langle 1\bar{1}0 \rangle$ uniaxial reconstruction of clean Au(111).¹¹ The full Xe monolayer on Pt(111) is, however, rotated by $\sim 3.3^\circ$ and has within 1% an identical lattice constant with the Xe bulk at the same temperature.¹² As shown here for the first time, the rotated layer is buckled. This buckling may be assigned to one of the equilibrium configurations of Fuselier, Raich, and Gillis⁹: Those Xe atoms which sit in threefold hollow sites are located deeper than the others. It is noteworthy that this type of "out of plane" distortion of the monolayer does not seem to be detrimental to the type-1 growth. The buckling vanishes gradually with the layer-by-layer thickening of the Xe film.

The data presented here have been obtained by

high-resolution He scattering. It has been demonstrated recently that this approach is particularly suited for the investigation of the structure¹² and dynamics¹³ of rare-gas films. Besides good angular and energy resolution, thermal-He scattering has some specific virtues of importance: characterization of substrate surface perfection down to defect and impurity densities of 0.1%, no disturbance even of very labile films, and applicability with any substrate.

We have extended here the capabilities of He scattering to characterize the growth of rare-gas films. Both the completion of the first and of the second monolayer and the degree of flatness of the whole film can be directly inferred from inelastic and diffuse elastic He scattering, respectively, i.e., from time-of-flight (TOF) spectra. This is exemplified in Fig. 1. The spectra show that the energy gain (and loss) of He

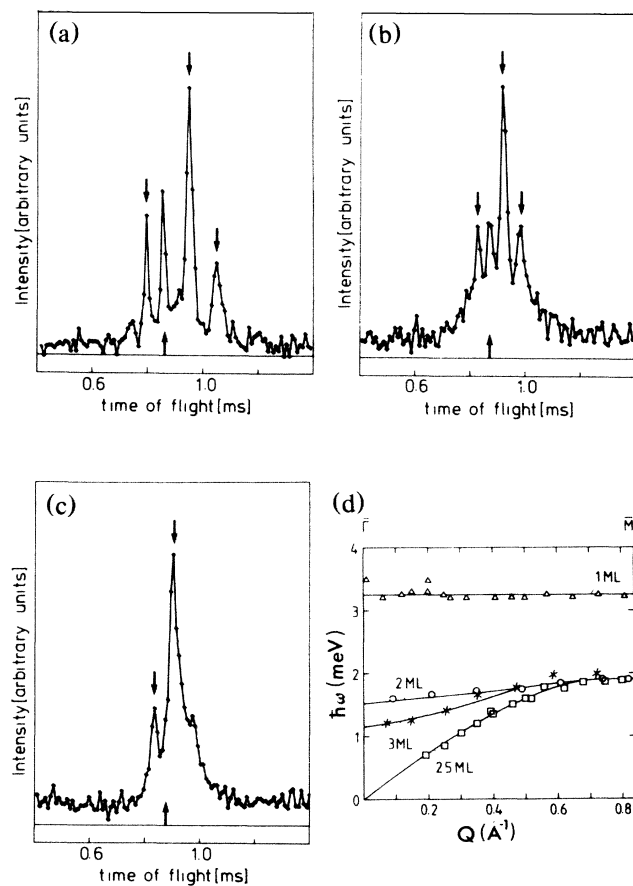


FIG. 1. He TOF spectra from Xe films on Pt(111): (a) 1 ML; (b) 2 ML; (c) 25 ML; and (d) phonon dispersion curves (trilayer included). All spectra (measuring time 15 min) are taken in the $\bar{\Gamma}\bar{M}$ direction with a beam energy of 17.7 meV, at an incident angle $\theta_i = 42^\circ$ ($\theta_f = 48^\circ$), a TOF path of 79 cm, and a surface temperature $T_s = 25$ K. The position of the diffuse elastic peak is indicated by an arrow pointing up.

atoms scattered from the Xe monolayer [Fig. 1(a)] is 1.8 to 2 times larger than in the bilayer case [Fig. 1(b)] throughout the Brillouin zone [Fig. 1(d)]. This large energy difference between monolayer and bilayer phonons makes it easy to detect the appearance of second-layer Xe atoms and thus to determine the completion of the monolayer with an accuracy of a few percent. The new procedure has also the advantage that it can be used at any temperature, i.e., also at that of the film growth experiment; no thermomolecular pressure² or other type of corrections are necessary. The same procedure can be applied to derive also the completion of the bilayer. The scanning curve has only to intersect the bilayer and trilayer dispersion curves in the left part of the Brillouin zone, where the phonon energies are different [Fig. 1(d)]. The exposures needed to complete the first and the second monolayer, respectively, appear to be equal within the experimental accuracy. This confirms for the second monolayer on Pt the constant sticking probability assumption made previously for all layers on graphite.²

In the TOF spectra in Figs. 1(a) and 1(b) the *diffuse* elastic peak, marked by an arrow pointing up, is clearly visible. This peak originates from scattering at impurities and defects and is considered as a sensitive indicator for surface disorder. From the comparison with TOF spectra taken from surfaces where the degree of disorder is known, one may infer that the monolayer is well and the bilayer even better ordered. The diffuse elastic peak is practically absent in the TOF spectrum in Fig. 1(c) taken from the 25-ML-thick Xe film [a similar behavior has been previously observed for a thick Xe film on¹³ Ag(111)]. This shows that the thick film is very flat, substantially flatter than the first layers, and thus that Xe on Pt(111) exhibits type-1 growth. This is not the only argument (see below), but a compelling one.

The structure of the various Xe layers < 1 ML thick growing on Pt(111) has been recently analyzed.¹² A commensurate $(\sqrt{3} \times \sqrt{3})R30^\circ$ and an incommensurate, but equally $R30^\circ$, structure are formed for submonolayer coverages at $T_s \geq 62$ and ≤ 58 K, respectively; both have the structure of the (111) surface of an fcc crystal, and differ mainly by their lattice constant d_{Xe} . The Xe structures being 30° rotated with respect to the Pt(111) substrate, their $\langle 11\bar{2} \rangle_{Xe}$ direction is coincident with the $\langle 1\bar{1}0 \rangle_{Pt}$ direction of the substrate. When the coverage is increased the Xe domains rotate up to $\phi = \pm 3.3^\circ$ with respect to $R30^\circ$ orientation. The azimuthal scan for the full monolayer [1 ML in Fig. 2(b)] shows this situation. The double peak arises from a nearly equal number of domains which are $R33.3^\circ$ and $R26.7^\circ$, respectively. The polar scans in Fig. 2(a) are measured with the scattering plane oriented $\phi = -3.3^\circ$ with respect to the $\langle 1\bar{1}0 \rangle_{Pt}$ direction, i.e., these are polar scans in the $\langle 11\bar{2} \rangle_{Xe}$

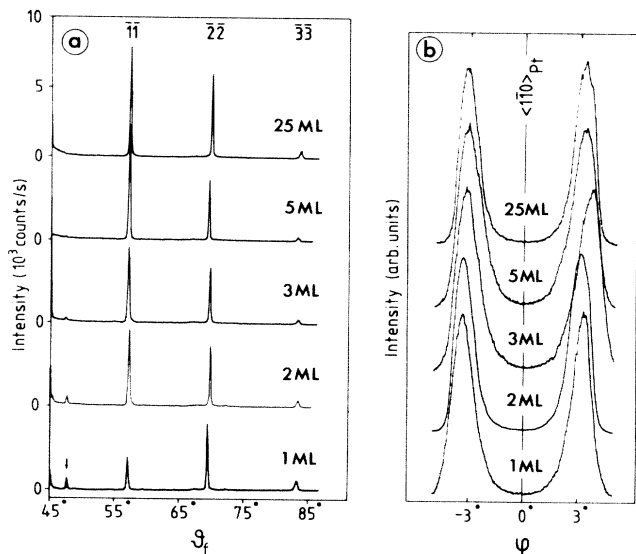


FIG. 2. (a) Polar and (b) azimuthal diffraction patterns of Xe films of indicated thickness. The incident plane for the polar patterns was oriented through the left-hand peaks in the azimuthal patterns (see text). The azimuthal patterns represent the $(\bar{2}, \bar{2})_{Xe}$ peaks. All patterns were taken with the $\theta_i + \theta_f = 90^\circ$ scattering geometry and with a He beam energy of 17.1 meV at $T_s = 25$ K. All polar patterns are plotted at the same scale; the azimuthal patterns are normalized.

direction of the $R26.7^\circ$ domains. The diffraction peaks are indexed with respect to these Xe domains (see also Ref. 12).

From the 1-ML scan in Fig. 2(a), $d_{Xe}^R = 4.34 \pm 0.03$ Å is obtained. This corresponds to a 9.6% misfit with respect to the $\sqrt{3}$ lattice constant; the rotation of $\phi = -3.3^\circ$ measured for the same layer is in agreement with the Novaco-McTague prediction.⁸ From the peak widths of the polar and azimuthal 1-ML scans an average domain size of about 300 Å is estimated. The apparent larger peak width in the azimuthal scan is an instrumental artifact due to the fixed scattering geometry, $\theta_i + \theta_f = 90^\circ$.¹⁴

The set of polar and azimuthal scans in Figs. 2(a) and 2(b), respectively, are measured at 25 K on 1-, 2-, 3-, 5-, and 25-ML Xe films. All films are deposited at 25 K at a 3D Xe pressure of 7×10^{-8} mbar. The completion of the first two layers has been determined from the phonon spectra as described above. The thickness of the consecutive layers has been estimated from the Xe exposure by invoking of the constant sticking probability assumption.² The layer structures seen in Fig. 2 grow during the deposition at 25 K. A subsequent layer annealing at 50 K (just below sublimation) leads to an increase in domain size.

The azimuthal plots in Fig. 2(b) show that all consecutive layers growing on the first ML are also rotated by $\phi = \pm 3.3^\circ$. Lattice constant and average domain

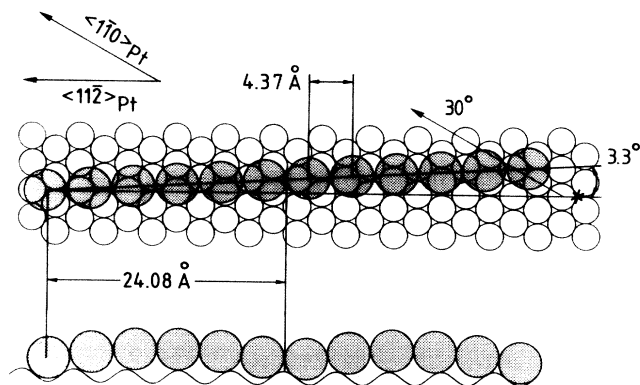


FIG. 3. Upper and side view of a 3.30° rotated domain of the full Xe monolayer; the open and shaded circles are the Pt and Xe atoms, respectively; the Xe domain is represented schematically by a chain of twelve Xe atoms (see text).

size deduced from the polar plots in Fig. 2(a) are also unchanged, e.g., $d_{Xe}^b = 4.33 \pm 0.03$ Å and ~ 300 Å, respectively, for the 25-ML film. The only significant difference in diffraction intensity ratios is between the 1-ML film and all others. This is probably mainly due to the influence of the Pt substrate on the He-surface scattering potential.

The sharp feature marked by an arrow in the 1-ML pattern in Fig. 2(a) is of particular interest. The position of this peak corresponds to a superstructure with a period of 23 ± 2 Å, which can be assigned to a buckling of the Xe layer. As already mentioned, the analysis of Fuselier, Raich, and Gillis⁹ shows that the orientational ordering predicted by Novaco and McTague corresponds to the locking of the adsorbed layer by a certain fraction of adsorbed atoms sitting in high-symmetry sites. The incommensurate rotated layer is, in fact, a layer with a higher order of commensurability. If this is true, the Xe atoms sitting in symmetry sites, probably in threefold hollow ones, are located somewhat deeper than the other Xe atoms and thus a buckling of the first monolayer has to be expected. The higher-order commensurability is thus directly accessible to a He scattering measurement.

The (23 ± 2) -Å period is compatible with both $5 \times d_{Xe}^R = 21.70 \pm 0.15$ Å and $\frac{1}{2} \times 11 \times d_{Xe}^R = 23.87 \pm 0.17$ Å. As the latter situation results in a better agreement with the data, we will discuss it in some detail by means of Fig. 3. We represent for simplicity a Xe domain by only one chain of twelve Xe atoms. Let us assume that the domain rotates around one Xe atom (here the first Xe atom from the left) and that the Xe atoms have a definite preference for either fcc or hcp threefold hollow sites. Before rotation, e.g., in the commensurate $(\sqrt{3} \times \sqrt{3})R30^\circ$ structure, the Xe atom chain is oriented along the $\langle 11\bar{2} \rangle_{Pt}$ direction, with each Xe atom sitting in an equivalent threefold

hollow site: The corresponding position (marked by an asterisk in Fig. 3) of the last Xe atom is $11 \times d_{Xe}^{\sqrt{3}} = 52.80 \text{ \AA}$ from the rotation center. When the coverage is increased (i.e., d_{Xe} decreased), and the domain starts to rotate, all Xe atoms except the first one leave their sites. According to Ref. 9, each Xe atom moves along a line oriented 30° with respect to the original orientation of the chain ($\langle 11\bar{2} \rangle_{Pt}$). After the domain (viz., the chain) has rotated 3.30° [the experimental value from Fig. 2(b)], the last Xe atom has reached exactly the nearest preferred threefold hollow site. This is the situation sketched in Fig. 3. The distance to the central Xe atom is now 48.08 \AA and the lattice parameter $4.37 \text{ \AA} = 48.08/11 \text{ \AA}$, in agreement with the experimental value. The actual buckling period is not 48.08 \AA (also in good agreement with the experimental $23 \pm 2 \text{ \AA}$) because, as obvious from Fig. 3, the fifth and the sixth Xe atoms are at less than 0.25 \AA from a preferred site and thus located nearly as deep as the first and last Xe atom. (The lower drawing in Fig. 3 suggests very schematically how the buckling comes about.) By repeating the argument for a chain of six Xe atoms one gets 4.33 and $21.64 \text{ \AA} = 5 \times 4.33 \text{ \AA}$ for the lattice parameter and the buckling period, respectively, both in agreement with the experiment, but 3.67° for the domain rotation, which is outside the experimental error limits. Thus the situation shown in Fig. 3 represents probably more accurately the structure of the full Xe monolayer.

Even this crude estimation makes it plausible that the buckling seen in the diffraction patterns originates from stronger bound Xe atoms located in symmetry sites. This suggests that the strain induced in the first monolayer by strong substrates via the density increase⁴⁻⁶ may be effectively counterbalanced by the same strong substrates locking in a fraction of the adatoms in symmetry sites. As a result, the complete wetting range on the scale of substrate strength may be substantially extended towards strong substrates as the Xe/Pt(111) results demonstrate. The incomplete wetting behavior of Xe on Au(111),⁴ in fact, supports this argument: The uniaxial reconstruction of¹¹ Au(111) impedes the formation of a layer with a higher order of commensurability, i.e., the locking of a substantial fraction of Xe atoms in symmetry sites.

The very gradual disappearance of the "buckling" peak (it can be seen even on the 5-ML pattern) is an additional argument for the type-1 growth.

In summary, Xe exhibits complete wetting on Pt(111)—a strong substrate—down to 25 K. Up to at least 25 ML, extremely flat Xe films consisting of $\sim 300\text{-\AA}$ domains grow epitaxially on a monolayer rotated $\phi = \pm 3.3^\circ$ with respect to the commensurate $(\sqrt{3} \times \sqrt{3})R30^\circ$ orientation. The monolayer is buckled with a period of $23 \pm 2 \text{ \AA}$. Rotation angle, misfit, and buckling period are in agreement with the Novaco-McTague prediction⁸ and the "coincident site lattice" concept of Fuselier, Raich, and Gillis.⁹ It is suggested that this effect contributes to complete wetting on strong substrates. High-resolution He scattering appears to be unique in the monitoring of the flatness of the film and in determination of the completion of the first two monolayers.

¹M. Bienfait, Surf. Sci. **162**, 411 (1985).

²J. L. Seguin, J. Suzanne, M. Bienfait, J. G. Dash, and J. A. Venables, Phys. Rev. Lett. **51**, 122 (1983).

³M. Bienfait, J. L. Seguin, J. Suzanne, E. Lerner, J. Krim, and J. G. Dash, Phys. Rev. B **29**, 983 (1984).

⁴J. Krim, J. G. Dash, and J. Suzanne, Phys. Rev. Lett. **52**, 640 (1984).

⁵R. J. Muirhead, J. G. Dash, and J. Krim, Phys. Rev. B **29**, 5074 (1984).

⁶D. A. Huse, Phys. Rev. B **29**, 6985 (1984).

⁷F. T. Gittes and M. Schick, Phys. Rev. B **30**, 209 (1984).

⁸A. D. Novaco and J. P. McTague, Phys. Rev. Lett. **38**, 1286 (1977), and Phys. Rev. B **19**, 5299 (1979).

⁹C. R. Fuselier, J. C. Raich, and N. S. Gillis, Surf. Sci. **92**, 667 (1980).

¹⁰B. Poelsema, L. K. Verheij, and G. Comsa, Surf. Sci. **152/153**, 851 (1985).

¹¹See, e.g., K. Takayanagi, Ultramicroscopy **8**, 145 (1982); U. Harten, A. Lahee, J. P. Toennies, and Ch. Wöll, Phys. Rev. Lett. **54**, 2619 (1985).

¹²K. Kern, R. David, R. L. Palmer, and G. Comsa, Phys. Rev. Lett. **56**, 620 (1986).

¹³K. D. Gibson and S. J. Sibener, Phys. Rev. Lett. **55**, 1514 (1985).

¹⁴R. David, K. Kern, P. Zeppenfeld, and G. Comsa, to be published.

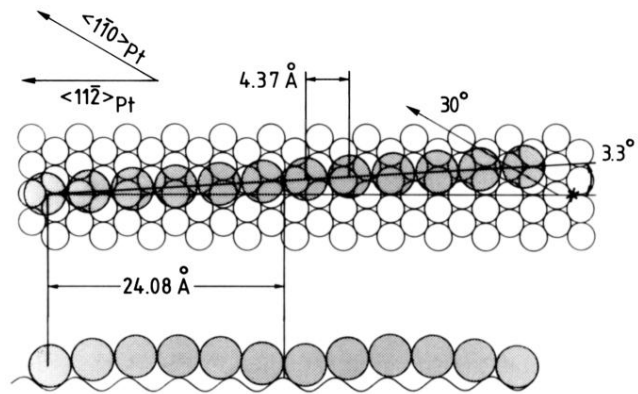


FIG. 3. Upper and side view of a 3.30° rotated domain of the full Xe monolayer; the open and shaded circles are the Pt and Xe atoms, respectively; the Xe domain is represented schematically by a chain of twelve Xe atoms (see text).